Into the dirt: datasets of sewer networks with aerial and ground platforms

David Alejo[1]
daletei@upo.es

François Chataigner[2]
francois.chataigner@eurecat.org

Daniel Serrano[2]
daniel.serrano@eurecat.org

Luis Merino[1]
lmercab@upo.es

Fernando Caballero[1]
fcaballero@upo.es

[1]**Service Robotics Laboratory**
Universidad Pablo de Olavide
Crta. Utrera, km. 1, 41013, Sevilla, Spain

[2]**Unit of Robotics and Automation,**
Eurecat, Centre Tecnològic de Catalunya,
Av. Universitat Autònoma, 23,
08290 Cerdanyola del Vallès, Barcelona, Spain

Abstract

This paper presents an unprecedented set of data in a challenging underground environment: the visitable sewers of Barcelona. To the best of our knowledge, this is the first dataset involving ground and aerial robots in such scenario: the SIAR ground robot and the ARSI aerial platform. These platforms captured data from a great variety of sensors, including sequences of RGB-D images with their onboard cameras. The set consists of fourteen logs of experiments that were obtained in more than ten different days and in four different locations. The complete length of the experiments in the dataset exceeds five km. In addition, we provide the users with a partial ground-truth and baselines of the localization of the platforms, which can be used for testing their localization and SLAM algorithms. We also provide details on the setup and execution of each mission and a partial labeling of the elements found in the sewers. All the data were recorded by using the rosbag tool from Robot Operating System (ROS) framework. Our goal is to make the data available to the scientific community as a benchmark to test localization, SLAM and classification algorithms in underground environments. The dataset are available at https://robotics.upo.es/datasets/echord.

1 Introduction

The idea of deploying autonomous robots into underground confined spaces like tunnels, sewers, mines and others is becoming more and more popular (an indicator for this interest is the current DARPA Subterranean Challenge[1]). The motivation is threefold. First, it would reduce labor risks, as it prevents operators from entering into such spaces, in which health hazards are common. Second, the use of an autonomous system would allow us to acquire more data that could be employed to perform a great variety of tasks, including accurate 3D-mapping of the environment, automatic detection of structural defects on the environment, such as holes or cracks. Last, the use of such systems can reduce human costs involved in the inspection and increase the productivity of the inspection procedure.

[1] https://www.darpa.mil/program/darpa-subterranean-challenge

However, the development of autonomous robots able to inspect this type of environments faces many challenges in several robotic areas such as perception, localization, navigation and communications. At the same time, performing tests in confined spaces is costly and has to be allowed by the local authorities as it requires qualified operators, specifically trained to enter in such spaces. For these reasons, we believe that the publication of datasets specifically gathered in such scenarios can be of great use to the scientific community.

In recent years, the scientific community, and the robotic community in particular, has published a wide variety of datasets that have become essential to develop, to test and to compare perception, learning, SLAM and planning techniques, to name a few. These datasets have been recorded in outdoors scenarios for developing perception algorithms for autonomous driving offering sensing data from different sources such as cameras and lidars. They include the KITTI dataset (Geiger et al., 2013), which has been widely employed to test functionalities for different intelligent vehicles and robotics, like SLAM, visual odometry, road detection, etc; and the Oxford Robotcar Dataset that has been recorded in more than a year span and has data recorded during a great variety of weather conditions (Maddern et al., 2017). Other datasets have been recorded in indoors/outdoors scenarios for social navigation and people identification (Ramón-Vigo et al., 2014). They offer LIDAR and RGB-D images among their sensing data but also offer detailed labeling of the pose of the people in the surroundings of the robot. The MPRT dataset has been designed for testing SLAM algorithms outdoors (Blanco et al., 2009). It offers accurate ground localization ground truth by means of several GPS-RTK synchronized sensors. Finally, some indoor datasets make also use of RGB-D cameras as its main sensor unit. The most relevant examples are the NYU2 RGB-D (Nathan Silberman and Fergus, 2012), the TUM RGB-D dataset (Sturm et al., 2012) and the ICL-NUIM dataset (Handa et al., 2014). In these cases, the datasets were obtained without the use of robots, and the main focus was to provide the developers of SLAM systems with tools to test the accuracy of their approaches.

However, as far as we are aware of, there are no publicly available datasets recorded in confined spaces such as sewers and mines to this date. The closest dataset we have found publicly available was generated in the TEDUSAR project (Leingartner et al., 2016). In this dataset, different depth sensors and cameras were used and their data was used with state of the art mapping algorithms to produce 2D and 3D maps of highway tunnels in two simulated disaster scenarios. Unfortunately, only the data acquired of two experiments in the same scenario is available and RGB-D data was not available in one of them due to harsh weather conditions.

Most of the available datasets involving aerial platforms are recorded in outdoors scenarios for different applications. Urban applications are a field of interest with some datasets such as (Majdik et al., 2017) supporting the development of future urban application of these systems. In emergency scenarios, for instance, a few examples are available such as the dataset covering the Disaster City test center (Pellenz et al., 2010) and a dataset involving aerial and ground Search and Rescue robots (Balta et al., 2017) published in the context of the European project ICARUS. To the best of our knowledge there is a lack of datasets involving aerial vehicles in confined spaces. One of the very few examples is (Burri et al., 2016) providing a detailed dataset of aerial robots operating in an industrial setting.

This paper contributes with aerial and ground robot datasets for the application of robotic sewer inspection. The dataset has been recorded in the context of the Challenge for Urban Robotics within the European project ECHORD++ [2]. Its main aspects can be summarized as follows:

- It is publicly available on the website (Alejo et al., 2019).
- It uses two different platforms: a ground robot, SIAR; and an aerial robot, ARSI (see Figure 1).
- The data was acquired from different locations on the real sewer network of Barcelona, Spain.
- The data of each experiment is stored by using the well-known and de facto standard rosbag tool from ROS.

[2] `http://echord.eu/`

- It is composed of more than ten different experiments with a total duration of roughly ten hours of experiments and a total trajectory length of about five km.
- More than three million of RGB-D images from the onboard cameras were captured.
- It includes information from multiple sensors, including cameras, depth cameras, 2D lidars, gas sensors and Inertial Measurement Units (IMUs).

Figure 1: Platforms used to gather the data in the sewers. Left: SIAR platform. Right: ARSI platform.

The rest of the paper is organized as follows: Section 2 presents the main characteristics of the SIAR platform, while Section 3 specifies the information available in the datasets generated by the SIAR platform. Section 4 summarizes the main characteristics of the ARSI aerial platform, and Section 5 specifies the information available in the datasets obtained with the ARSI platform. Finally, Section 7 concludes the paper with a special emphasis on the lessons learned during the course of the experimentation in real sewers.

2 Overview of the SIAR platform

All the experiments presented in this paper that involve a ground robot were performed with the SIAR platform Version 3, which has been designed by IDMind company [3]. References to the previous version of the platform can be found in (Alejo et al., 2016). Figure 2 represents the platform with all its main characteristics. In particular, this platform is a six-wheeled ground robot with the ability to change the width between its wheels in order to address the different sections of the sewer network and to deploy or retrieve the robot through a manhole. The robot is fully equipped to move autonomously for about 4 hours while executing the inspection operation. Below, a list with the main specifications of the platform can be found.

[3] `https://idmind.pt`

Figure 2: SIAR robotic platform V3.

- Robot Kinematics: six wheeled with six independent locomotion motors. One linear motor for width control.
- Weight: 58 Kg.
- Battery autonomy: 4 hours.
- Maximum speed: 0.75 m/s.
- Acceleration: 1 m/s^2.
- Emergency stop acceleration: 3.3 m/s^2.
- Dimensions with maximum width (Height x Width x Length) : 44 x 70 x 84 cm.
- Dimensions with minimum width (Height x Width x Length): 44 x 50 x 98 cm.

The SIAR platform is equipped with an IMU, one encoder for each traction motor and one extra sensor to estimate the position of the linear motor for width adjustment. In addition, a robotic arm with five degrees of freedom (DoF) is installed in the rear part of the platform. This arm was designed to deploy and to collect communication systems to use them as repeaters over the course of the experiments. However, in the experiments presented here, the repeaters were deployed manually.

2.1 Equipped sensors

The SIAR ground platform can be equipped with a great variety of sensors due to its available payload. In this section, we detail the sensors onboard the SIAR platform in the dataset.

2.1.1 RGBD cameras

We opted for using structured light RGB-D cameras as they are very convenient for performing 3D scans of the surroundings of the robot even without the presence of illumination. These kind of cameras emit an IR pattern that is projected onto the scene. This pattern is then sensed by an IR camera and the depth can be estimated by triangulation (Smisek et al., 2013). In particular we use both Astra and Astra S devices from Orbbec Ltd (see Figure 3). However, in our view these devices have three main drawbacks. First, they are not capable of estimating the distance of objects that are closer than a given distance, which is approximately 45 cm for Astra cameras and 35 cm for Astra S cameras. Another drawback is their limited Field of View (FoV), which of 60 horizontally in the Astra devices. Finally, as they have to sense the light emitted by its IR projector, their performance can be degraded in outdoors because of the sunlight. Obviously, this third point is not an issue in the sewer environment.

Figure 3: Astra S RGB-D camera from Orbbec Ltd.

To overcome the FoV issue, we opted for placing an array of cameras that covers the most relevant sensing zones for navigation and operator awareness. Figure 4 shows the disposition of the array of cameras as installed in the SIAR platform. In contrast to the most common rig of cameras, in which each camera is distributed symmetrically (see the camera rig of eight cameras presented in (Fernández-Moral et al., 2014) as an example), we have designed a rig of cameras in which each one has a specific purpose. Next we detail the main purpose of each camera:

Figure 4: Disposition of the cameras in the SIAR V3 prototype.

- Two Astra cameras for operator awareness and for 3D reconstruction. These two cameras (front and rear) are placed horizontally and can provide long-range information (up to 8 m) that are used by localization and navigation algorithms. The cameras have the following ROS prefix to their produced images: `/front` and `/back`.
- Four Astra S cameras (two front and two rear) tilted 45 degrees (Figure 5 left) downwards for gathering information of the floor in the surroundings of the SIAR platform. Two cameras are

needed due in order to extend their FoV. By using the two cameras (Figure 5 right) is possible to have a combined 110 FoV in each direction (backwards and forwards). The combined FoV is slightly lower than the sum of two cameras, to avoid blind areas. The information of these cameras is used for reactive navigation as well as to increase operator awareness. This information is critical to guide the robot safely across the sewers. Also they can be of great use to detect and precisely localize serviceability problems in the sewer system. The cameras have the following ROS prefix to their produced images: `/front_left`, `/front_right`, `/back_left` and `/back_right`.

- One Astra S camera pointing to the ceiling. This camera is used to reliably detect the manholes of the sewers, improving the performance of the localization system of the SIAR platform (Alejo et al., 2017). In addition, the camera can also be used to extract 3D information of the ceiling whenever required. The ROS prefix of this camera is `/up`.

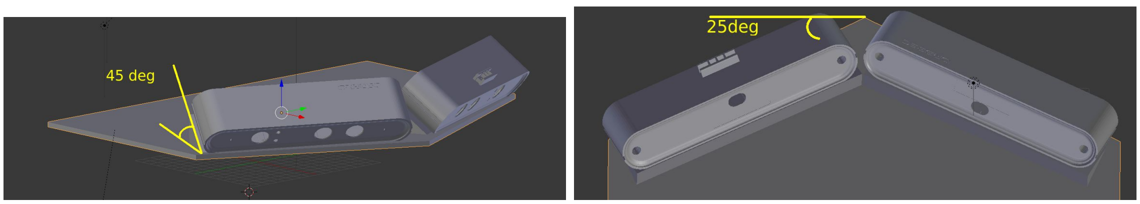

Figure 5: Left: tilt angles of the sensors pointing downwards. Right: top view of the sensing system, the yaw angle with respect to the horizontal of the robot is marked.

2.1.2 IMU

We have integrated the unexpensive ArduIMU v3 IMU device (see Figure 6 left) into the SIAR platform and we have placed it near the center of rotation of the robot. It incorporates the Invensense MPU-6000 MEMS 3-axis gyro and accelerometer as well the 3-axis I2C magnetometer HMC-5883L that provide us with high quality IMU data. This data is further filtered with our opensource arduIMU ROS package[4].

2.1.3 Gas sensors

A Waspmote Pro OEM gas system was installed on the robot to measure the concentrations of relevant gases inside the sewers. Figure 6 right shows the Waspmote Pro system.

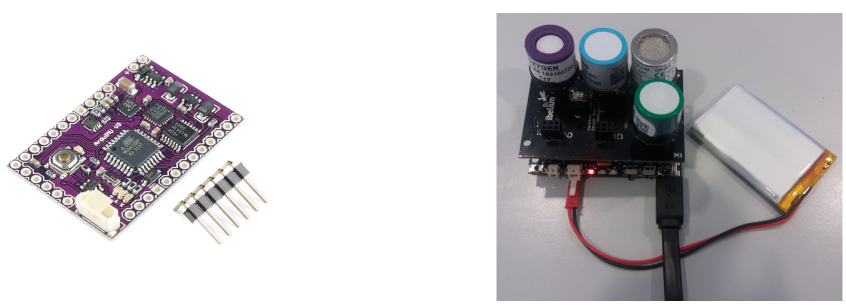

Figure 6: Left: ArduIMU v3 system (picture from from https://cdn.sparkfun.com under license CC BY 2.0). Right: Waspmote Pro OEM gas system.

The gas sensor can measure Molecular Oxygen (O2), Carbon Monoxide (CO), Hydrogen Sulfide (H2S), Methane (CH4) and Combustible gases. The system also includes a temperature (C), humidity (% RH),

[4] `https://github.com/robotics-upo/arduimu_v3`

pressure sensor (Pa) that can be used to increase the accuracy of the gas sensors. We use our open source Libelium waspmote ROS package[5] that interfaces and parses the data generated by the gas sensor.

3 SIAR Data details

This section makes a description of the data that is presented in the experiments with the ground platform. We divide the available data into two main sets. First, the data acquired in the experiment is listed in Section 3.1. In addition, we provide information that can be used as baseline or partial ground truth for localization algorithms, as explained in Section 3.2.

3.1 Sensor data details

All rosbag files in the dataset include the topics or sources of information that are acquired by the sensors onboard the platform or inferred in real-time from it. For details about the information avoilable in the custom data types, please refer to Appendix A.

- `/odom` This topic contains the odometry as estimated by the platform with the encoders of the wheels and the onboard IMU. Standard datatype used: `nav_msgs::Odometry`.
- `/siar_status` This topic contains basic information of the SIAR platform. Standard datatype used: `siar_driver/SiarStatus`
- `/tf` This topic contains the relative transformations between the static coordinate frames using the standard data type `tf2_msgs::TFMessage`.
- `/rssi`. This topic contains the RSSI information of the communication system onboard the robot. This topic uses the custom message data type `rssi_get/Nvip_status`.
- For each a RGB-D camera with prefix `camera` the rosbag contains the following topics as provided by the OpenNI2 ROS driver[6]:

  `/camera/depth_registered/camera_info`. This topic contains the calibration parameters of the IR camera. It uses the Standard data type `sensor_msgs::CameraInfo`.

  `/camera/depth_registered/image_raw/compressed`. This topic contains the compressed depth image as obtained with the sensor. It uses the standard data type `sensor_msgs::CompressedDepth`.

  `/camera/rgb/camera_info`. This topic contains the calibration parameters of the RGB camera. It uses the standard data type `sensor_msgs::CameraInfo`.

  `/camera/rgb/image_raw/compressed`. This topic contains the compressed RGB image as obtained with the sensor. It uses the standard data type `sensor_msgs::CompressedImage`.
- `/gas_info`. This topic contains the measurements made by the onboard gas sensor. They are available only in some experiments, such as the presented in Section 6.5.6.

3.1.1 Coordinate frames

In this section, we detail the coordinates frames that appear in the log of the experiments. Figure 7 represents the spatial disposition of the frames over the SIAR platform. The transforms that relate the different frames are recorded into the rosbag files by using the ROS tf package[7].

[5] https://github.com/robotics-upo/libelium_waspmote_gas_node
[6] https://github.com/ros-drivers/openni2_camera
[7] http://wiki.ros.org/tf

In the SIAR system, the coordinate frames can be divided into the following families of frames.

- **Robot frame:** `/base_link`. This frame has as origin the center of the axis of the wheels in the middle and it is placed on the floor level. In addition, we provide the frame `electronics_center`, which lies in the center of gravity of the electronics box. Its position depends on the state of the width adjustment mechanism.
- **Odometry:** `/odom`. It lies in the position of the robot when the odometry module is activated for the first time.
- **Camera frames.** Each RGBD camera has five links associated. The one at the center of the camera is named `camera_link`, where the word "camera" should be replaced with the actual name of the camera. In addition, there are two links for each sensor included in the camera (IR and RGB): `camera_rgb_frame`, `camera_rgb_optical_frame`, `camera_depth_frame`, `camera_depth_optical_frame`. These links are provided by the openni2_camera driver. Figure 8 depicts the whole family of frames of the back cameras as well as the parent frame of each other camera in the system.
- **Arm frame:** `/siar_arm`. There are a family of coordinate frames that are used for determining the position of each link of the arm. The final frame is related with the position of the camera installed in the end-effector of the arm.
- **Global frame:** `/world`. This transform relates the local reference frame used in ROS with the global coordinate system using the ENU convection (east-north-up). The baseline trajectories are given with respect to this frame.

We want to point out that we automated the process of calibrating the transform of relative poses between cameras (usually known as extrinsical calibration of an array of cameras). Most methods rely on external and accurate position systems (Avetisyan et al., 2014), while other are based on estimating the ego-motion of the set of cameras using SLAM or Visual Odometry (Heng et al., 2015)(Schneider et al., 2013). However, they tend to be computationally expensive and may present observability issues. We use the method proposed in (Fernández-Moral et al., 2014), which is based on estimating planar surfaces with the depth information of different cameras and obtaining the transform that makes them match. We also use this method to calibrate the transform between the `base_link` of the robot with the `front_camera_link`. To this end, we place the platform in such position that we know the poses of three nearby planes with respect to the robot (see Figure 9).

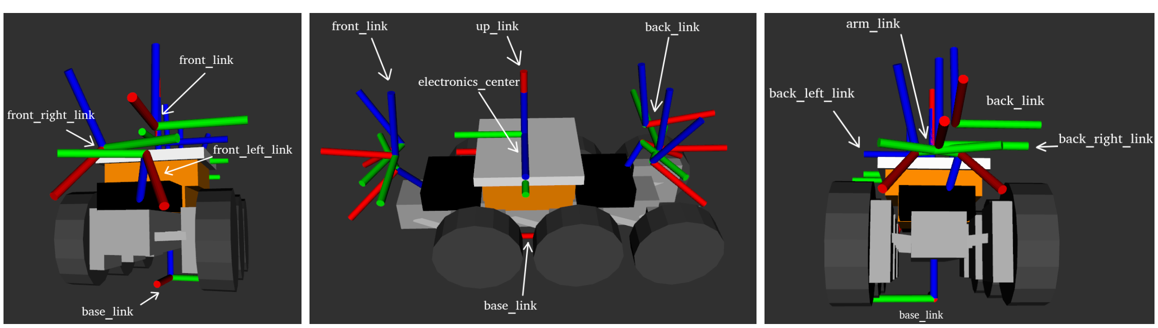

Figure 7: 3D visualization of the coordinate frames. Left: frontal view. Middle: cenital view. Right: rear view.

3.2 Ground truth

We provide the user with data for testing the accuracy of localization algorithms. In particular, we offer the following pair of topics in this regard.

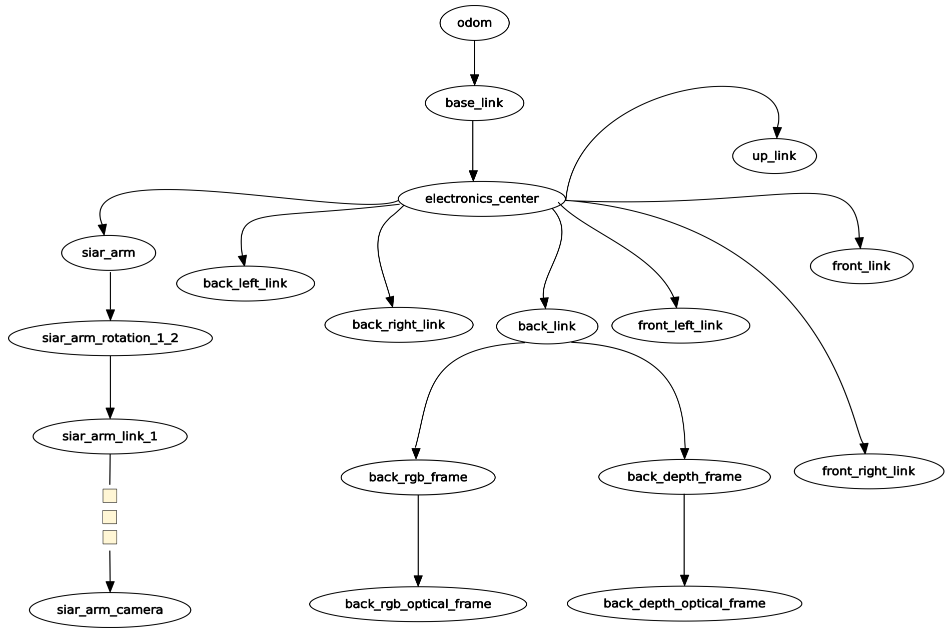

Figure 8: Simplified transform tree of the system that relates the different coordinate frames.

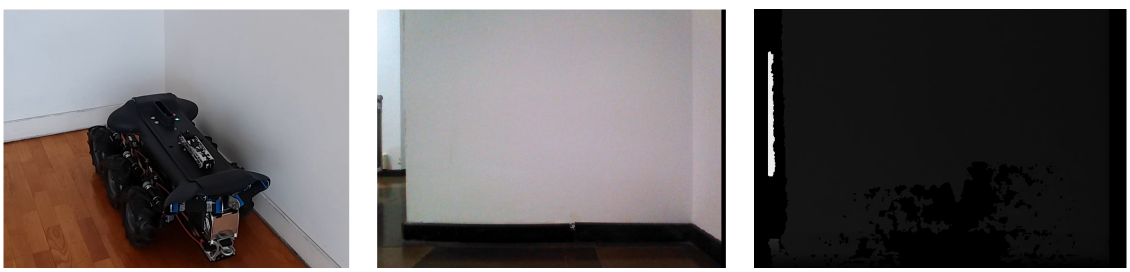

Figure 9: Left: Proposed disposition to automatically estimate the transform from the `base_link` frame to the `front_camera_link`. Middle-right: RGB and depth images obtained from such position.

- `/manhole`. This topic has as type `manhole_detector/Manhole` (see Appendix A) and it is emitted whenever the platform passes below the manhole. These instants have been manually labeled in each experiment, as they could be easily obtained from the images of the upward facing camera. This information can be used as ground truth as these elements are precisely localized with the help of the provided Geographic Information System (GIS).

- `/baseline`. This topic has `geometry_msgs/Pose` as type and it contains the reference trajectories followed by the SIAR system. These trajectories have been calculated by using the particle filter based localization method described in (Alejo et al., 2017) with the following adjustments:

  - We increased the population of the particle filter to the range [1200-1500].
  - We disabled the Convolutional Neural Network(CNN)-based manhole detector. It was replaced by perfect manhole detection whenever the robot passed below a manhole.
  - In some cases, we reduced the GIS data in order to only consider the places actually visited by the platforms.

4 Overview of the ARSI platform

The experiments involving the Micro Aerial Vehicle (MAV) were performed with two prototypes developed by the ARSI (Autonomous Robot for Sewer Inspection) consortium. In the following sections they are referred to as "V2" and "V3". Figure 10 depicts the ARSI V3 MAV prototype.

The ARSI MAV is a compact quadrotor designed specifically for the operation in sewer sections as narrow as 70 cm (at ground level). The dimensions of the targeted sewer sections limits the maximum width of the frame, the maximum propeller size and thus the Maximum Take-Off Weight (MTOW). The MAV is lightweight and robust, with an estimated flight autonomy of 13 minutes and a payload capacity of 1 kg. It carries several onboard sensors, allowing it to execute autonomous inspections supervised by operators on the surface.

Figure 10: ARSI Micro Aerial Vehicle V3.

The main ARSI MAV features are the following:

- A quadrotor configuration with a carbon fiber frame.
- Overlapping 11" propellers to reduce the platform width.
- Dimensions (Height x Width x Length) : 31 x 62 x 81 cm.
- Weight: 3.5 kg including sensing payload and battery.
- Flight autonomy: 10 to 15 minutes depending on the sewer section.
- Average velocity during sewer inspections : 0.5 m/s.
- Contact tolerant thanks to the propeller protection specifically designed for the dynamics of sewer inspection.
- A wide landing structure to cope with the central canal present in most sewers.

4.1 Equipped sensors

The ARSI MAV payload includes an onboard autopilot for low-level control. Additionally, an Intel NUC onboard computer connected to a set of sensors for real-time localization and path planning. Finally, the platform is equipped with a high-bandwidth communication wireless device that links it with the control station at the surface.

The sensing configuration is shown in Figure 11. It includes a front-facing RGB-D (color and depth) camera for localization, a front-facing wide-angle HD camera for data collection, an horizontal 2D laser for reactive navigation along the sewer tunnels, and a down-looking range finder providing altitude measurements.

Since sewer inspections are typically carried out in complete darkness, the ARSI MAV uses a strip of LEDs to illuminate the scene, both to collect video data for inspection purposes and to navigate autonomously. ARSI V2 used LEDs with a maximum output of 1650 lm; these were upgraded to 3000 lm long-range LEDs in ARSI V3 in order to improve the image quality, in particular of the sewer roof.

RGB-D data from the camera is processed at on the onboard PC using the visual odometry algorithm RTABMAP (Labb and Michaud, 2018) to produce a real-time estimation of the MAV pose during flight. The laser's 360 degrees field of view allows the MAV to fly forward or backward. Backward flight was added in ARSI V3 typically to return to the deployment point after an inspection.

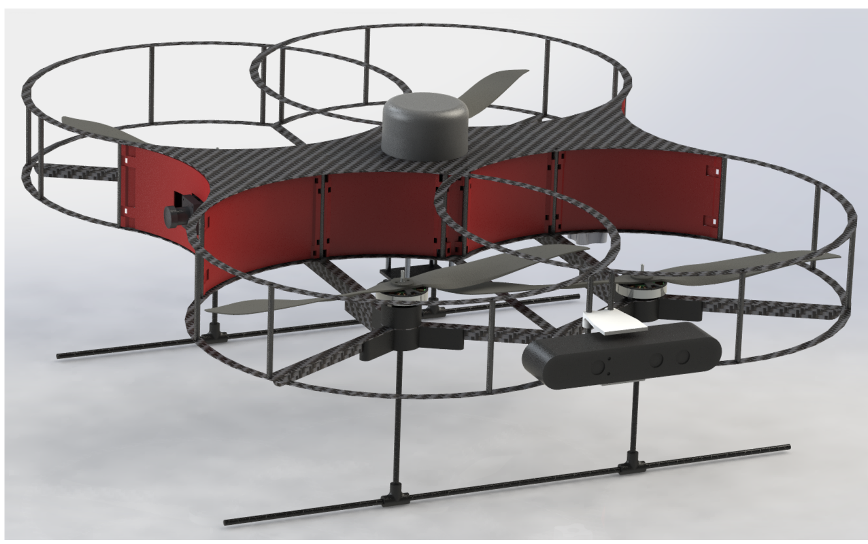

Figure 11: ARSI V3 design.

4.1.1 Pixhawk autopilot

The ARSI system uses a Pixhawk v1 autopilot (Meier et al., 2011) for low-level control and localization. Pixhawk is an open-hardware, low-cost autopilot running the PX4 open-source firmware (Meier et al., 2015) on the NuttX OS.

Data from the onboard accelerometers, gyroscopes and magnetometers (Invensense MPU 6000 and ST Micro LSM303D) are available in the datasets, together with the estimated attitude and heading.

PX4 includes estimators for attitude and local pose. The attitude estimator fuses inertial measurements with the external heading reference from the visual odometry, while the Local Position Estimator (LPE) implements an extended Kalman filter for 3D position and velocity estimation, using the visual odometry solution and altitude measurements. Both the estimated attitude and pose are available in the datasets.

4.1.2 RGB-D camera

Like the SIAR robot (see Section 2), a structured light RGB-D camera was selected as the main sensor for navigation in ARSI. Specifically, we use an Astra camera from Orbbec Ltd mounted at the front of the platform as shown in Figure 11.

The sensor has a maximum range of 8m, and produces images with a resolution of 640x480 (VGA). The ARSI MAV also carries a wide-angle HD frontal camera used for sewer inspection data collection.

4.1.3 2D laser scanner

A 2D laser mounted on top of the platform produces high-frequency range measurements to the nearby obstacles, in particular the sewer walls. This sensor is the main source of information for path planning and reactive navigation in the narrow sewer tunnels.

ARSI V2 used a Hokuyo UST-10LX rangefinder. This lightweight device (130 gr) has a field of view of 270 degrees and generates 2D scans at a frequency of 40 Hz. With a range of 10 m and an angular resolution of 0.25 degrees. The experiments in Section 6.3 incorporate data from this sensor.

In ARSI V3 we used the RPLidar A2 rangefinder (see Figure 12). This lightweight (190 gr) and low-cost sensor operates at 10 Hz with a maximum range of 12 m and an angular resolution of 0.9 degrees.

Despite a slight loss in performance in terms of resolution and frequency, our sensor choice was based on end-user requirements. In particular, they required the MAV to have the capability of flying backwards as well as forwards. The experiment carried out in Virrei Amat (see Section 6.4) includes data from the RPLidar A2.

Figure 12: Left: Hokuyo UST-10LX rangefinder from ARSI V2. Right: RPLidar A2 rangefinder from ARSI V3.

4.1.4 Altimeter

A distance sensor is mounted underneath the platform to measure the MAV altitude over the sewer floor. These measurements are integrated into the position estimation as the main source of information for the Z axis.

ARSI V2 carried a Teraranger One infrared sensor connected to the onboard PC. In this configuration, both raw and filtered altitude measurements are available in the dataset (see experiments in Section 6.3).

ARSI V3 carries the new Teraranger EVO short-range sensor connected directly to the Pixhawk autopilot. In this configuration, we could only record filtered range measurements. This applies to the experiments carried out in Virrei Amat (see Section 6.4).

5 ARSI Data details

This section describes the part of the dataset related to the ARSI aerial platform. As previously mentioned, the experiments published in this dataset correspond to two different configurations of the ARSI MAV. This section details the contents of the dataset, and specifies the differences in the data captured with each configuration.

5.1 Sensor data details

All rosbag files in the dataset include the topics listed below, acquired by the various sensors onboard the platform, or inferred in real-time from it. Data generated onboard the Pixhawk autopilot is received on the secondary telemetry port and stored in rosbag files as well.

- `/imu/raw_data`: raw data (accelerometers and gyroscopes) from the Pixhwak IMU without orientation. Datatype: `sensor_msgs::Imu`.
- `/imu/mag`: data from the Pixhawk compass. This built-in compass is severely affected by magnetic interference during operation in the sewers. Datatype: `sensor_msgs::MagneticField`.
- `/imu/data`: IMU orientation computation generated by the Pixhawk autopilot sensors. Uses the datatype `sensor_msgs::Imu`.
- `/teraranger`: distance from the Teraranger sensor to the ground. Datatype: `sensor_msgs::Range`
- `/scan`: 2D laserscan data. Datatype: `sensor_msgs::LaserScan`. As described in Section 4.1.3, different laser scanners were used on the ARSI MAVs. We added a prefix to this topic to indicate which laser model was used (`/hokuyo/scan` or `/rplidar/scan`).
- `/tf`: relative transformations between the coordinate frames. Datatype: `tf2_msgs::TFMessage`.
- `/front_camera/rgb/image`: RGB images produced by the Orbbec Astra RGBD camera, uses the datatype `sensor_msgs::Image`. In some experiments, the frame rate was reduced in order to manage storage limitations. In these experiments, the topic used is `/front_camera/rgb/image/throttle`.
- `/front_camera/rgb/camera_info`: it contains calibration parameters of the RGB camera. Datatype: `sensor_msgs::CameraInfo`.
- `/front_camera/depth/image`: depth images produced by the Orbbec Astra RGBD camera. Datatype: `sensor_msgs::Image`. In some experiments, the frame rate was reduced to manage storage limitations. In these experiments, the topic is called `/front_camera/depth/image/throttle`.
- `/front_camera/depth/camera_info`: calibration parameters of the IR camera. Datatype: `sensor_msgs::CameraInfo`.

5.1.1 Coordinate frames

The coordinate frames in the ARSI dataset are defined as follows:

- **Robot frame:** `/base_link`. This coordinate is centered on the Pixhawk autopilot. The actual reference point is marked on the Pixhawk unit.
- **Laser scanner:** `/laser`. It is located at the center of the 2D laser scanner.
- **RGBD camera:** `/openni_rgb_optical_frame`. Optical center of the RGB camera on the frontal Orbbec Astra device.

- **Altimeter:** `/teraranger`. It is located at the center of the distance sensor used as altimeter.
- **Odometry:** `/odom`. Real-time position and orientation of the MAV calculated using the visual odometry modules. The `/odom` origin references the location where the MAV is deployed in the sewers prior to takeoff.

5.2 Ground truth

For the aerial dataset, we provide the user with reference data to evaluate localization algorithms. In particular, we offer the following.

- `/rtabmap/odom`. This topic of type `nav_msgs/Odometry` contains the output of RTABMap algorithm running the RGBD odometry (Labb and Michaud, 2018).
- `/baseline/local_estimation/pose`. This topic of type `geometry_msgs/PoseStamped` contains the output of our local localization system as published by the Pixhawk autopilot after the fusion with IMU, RGBD odometry and altimeter data. This fusion uses the Local Position Estimator (LPE) of PX4.
- `/baseline/local_estimation/velocity`. Likewise, the velocity estimation is also published as `geometry_msgs/TwistStamped` message.
- `/baseline`. This topic of type `geometry_msgs/PoseStamped` contains the output of our global localization system (see Section 3.2).

6 Dataset

The dataset published in the webpage (Alejo et al., 2019) comprises the logs of nine different experiments with SIAR and three with ARSI. The experiments presented in the dataset were held in four (and counting) different scenarios. However, for the sake of brievity, we only describe here two different scenarios and six experiments. The duration of each experiment varies from half an hour to more than three hours in the case of the ground robot. In contrast, MAV flights are generally shorter experiments targeting one or two segments of the sewer network.

In our dataset we present the results of different trials in the same scenario, which can be very useful due to the following reasons:

- It allows the user to train machine learning algorithms with a set of data and validate the results with another set.
- Some issues that can appear during the execution of a mission are less critical, as more data of other experiments is available.

In our view, the presented dataset can be of great use for testing mapping and localization algorithms in real confined spaces. To help the researchers in this task, we provide them with global baseline trajectories (see Section 3.2). Additionally, partial ground truth information of the localization of the platform is given in the case of the experiments with the SIAR ground platform.

6.1 Experimental Setup

In this section we summarize the main steps which are necessary to have each platform working properly inside the sewer network.

6.1.1 SIAR experimental setup

Figure 13 depicts the setup of the experiments of the SIAR platform in the Mercat del Born scenario. To make the setup, we followed the same procedure in the experiments that were performed with the SIAR platform. The main procedure consisted of the following steps:

- **Robot deployment.** We deploy the robot configured at minimum width through a Manhole planned in advance. A winch is necessary to proceed with the deployment due to the weight of the platform (40 Kg approx.).

- **Deployment of the repeaters.** We deploy the communication device of the base station in the closest fork to the deployment manhole. In this way, we ensure network coverage over the two connecting streets. Three additional communication devices were deployed in the area to ensure network connectivity over the whole track (see Figure 13 and Figure 15).

- **Integrity checks.** First, our system checks that all the on-board cameras and sensing devices. Then, we also check have connectivity over all the deployed repeaters.

- **Mission execution.** In our system, the operator is always in control of the platform by sending high level commands to it such as advancing, going backwards or giving a new direction of exploration whenever a fork is found.

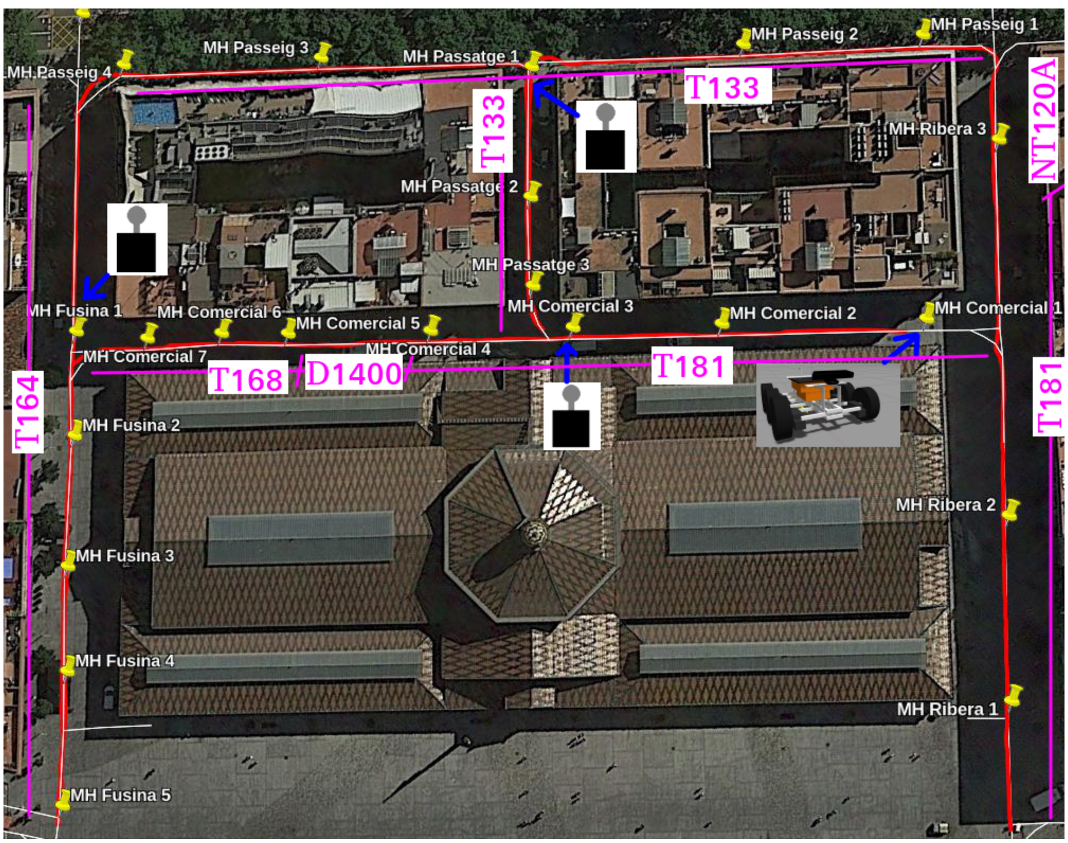

Figure 13: Experimental setup for the Scenario I in the experiments with the SIAR platform. The manholes where the communication devices and the platform were deployed are marked with blue arrows. The baseline trajectory for Experiment 3 is plotted in a red line. The cross sections are represented in purple.

6.1.2 ARSI Experimental setup

The inspection procedure for the ARSI system was as follows:

- **Mission planning:** missions representing individual MAV flights are planned in advance by operators using a dedicated user interface. Each mission is defined by an entry manhole where the MAV is deployed, a series of sewer segments to inspect, and an exit manhole where the MAV is recovered or where the battery is replaced before the next flight.
- **Deployment**: standard manholes in Barcelona have a diameter of 70cm. Both ARSI prototypes fit comfortably, and we were able to deploy them in the sewers very simply by using a rope with 3D-printed hooks for the MAV frame.
- **Communications**: live communications with the MAV during flights were implemented using an off-the-shelf 2.4GHz WiFi router mounted in a waterproof case. The router was deployed in the sewer at the entry manhole, where it is connected to the operator interface on the surface by means of an Ethernet cable. We took advantage of the long straight sewers where the WiFi signal carries very far because of the wave-guiding effect of the tunnels (Rizzo et al., 2018).
- **Flight execution**: while our system can execute missions autonomously, operators can also issue high-level commands such as pausing the MAV to observe an area of interest in the sewer, changing the inspection speed and the altitude, triggering an emergency landing, or flying backwards to return to the deployment point.

6.2 Scenarios

In this section, we describe some locations where the experiments were carried out. As stated before, we only describe with detail the experiments carried out in two areas: Mercat del Born and Virrei Amat squares. The reader is referred to the dataset website (Alejo et al., 2019) for the details on the remaining scenarios.

In each scenario, we provide the GIS by means of a KML[8] file that describes the topology of the sewer network as a connected graph. This graph has as vertices the manholes present in the sewer system, the forks present in the sewers and points were a sewer gallery changes its direction. The edges of the graph correspond to the sewer galleries. In addition, the graph has information about the ideal cross sections of each gallery.

6.3 Scenario I: Mercat del Born

Figure 13 represents the location of the Scenario I, which corresponds to sewers located at the Mercat del Born, Barcelona. The goal of the experiments was to visit the part of the sewer network marked in a red line. The total length of the track to be inspected is of about 640m.

In order to give a better idea of the environment where the experiments were carried out, the shape of the different sewer sections of this scenario is represented in Figure 14. Please note that their labels appear at each sewer segment in Figure 13.

We present the data obtained during four different experiments. In the three experiments with the SIAR ground platform, the whole track was almost entirely visited while the platform was operated from the surface. Therefore, the data of the seven RGBD cameras is available as there is no presence of an operator in the surroundings of the platform in its FoV. In the case of the ARSI aerial platform, the experiment was split into a series of flights due to the autonomy limitations.

[8] `https://developers.google.com/kml/documentation/kmlreference?hl=es`

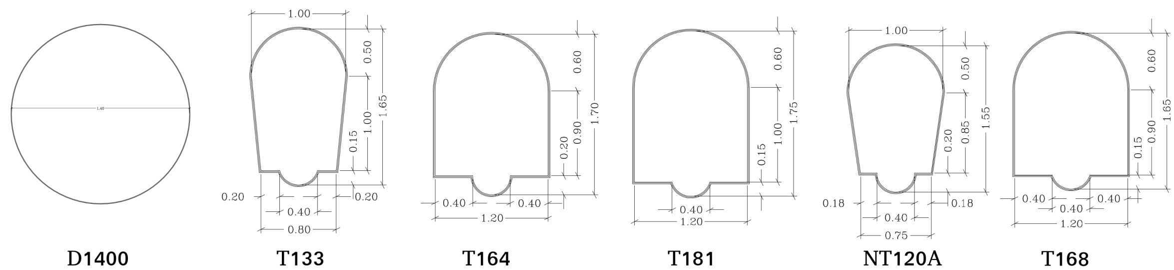

Figure 14: Transverse sections of the sewer gallery in Scenario I (Mercat del Born).

6.4 Scenario II: Virrei Amat Square

This scenario had a length of roughly 500m. Figure 15 represents the location where the experiments were carried out, as well as the deployment manholes of the ARSI system, the SIAR platform and their communication devices.

There are two long segments that have very similar cross sections (T111 and T114A). They are about 60 cm wide in the floor area (see Figure 16). In contrast, the last segment has not a uniform cross section. Its section varies from T158A to T141, which are noticeably wider when compared to the cross sections of the previous segments.

This track has been visited in three different experiments with the SIAR platform, which were carried out from the 27th of June to the 4th of July, 2018. Additionally, the ARSI platform made an experiment on the 3th of July, 2018. In this paper, we detail the results of the experiments carried out on 3th and 4th of July in Experiments 5 and 6, respectively. The reader is referred to the webpage of the dataset for obtaining information about the other experiments performed in this location.

6.5 Experiments

Finally, some of the experiments performed in both scenarios are described, focusing in their particularities.

6.5.1 Experiment 1: SIAR 2017-09-21

This was the first experiment in which the SIAR platform was operated from the surface by the operator. It was carried out in the Scenario I. Figure 17(left) represents the baseline trajectory of the platform in this experiment. In this case, we were able to operate the platform over the whole track from the surface, with the exception of a part of the Fusina street due to time constraints. The operators only needed to enter the sewer to deploy and to retrieve the robot, and to recover the robot when it fell to the gutter while handling the fork between Ribera street and Passeig Colom. The length of the inspected track exceeds 400 meters in Experiments 1, 2 and 4 and the platform was able to visit all the traverse sections represented in Figure 14.

6.5.2 Experiment 2: SIAR 2017-10-10

In this experiment, the autonomous mode was improved, allowing us to perform the whole track without any intervention inside the sewers in Scenario I. The baseline trajectory is represented in Figure 17(right). In this case, the log did not start in the deploy point due to technical issues. It started from manhole Fusina 2 in direction to manhole Fusina 5.

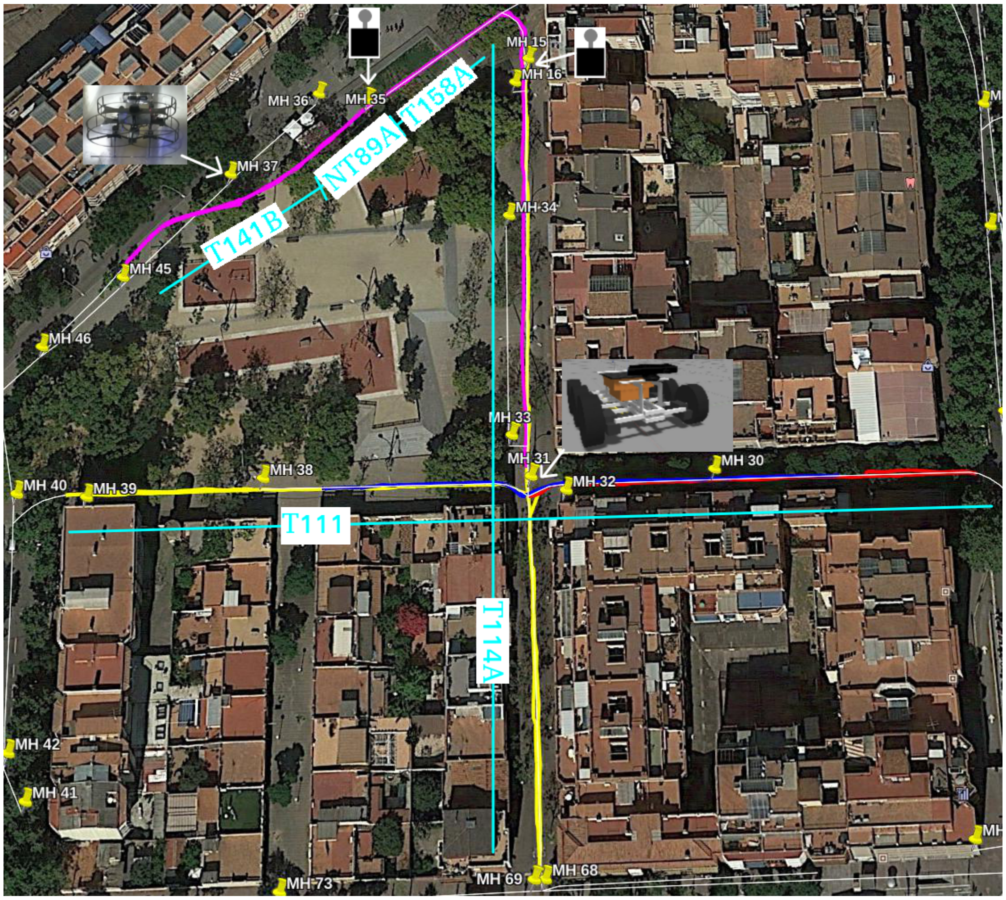

Figure 15: Location of Scenario 2 with the deployment manholes of ARSI, SIAR and their communication devices. Additionally, we depict the baseline trajectories of experiment 6. They were obtained in the following order: red, blue, yellow and purple.

6.5.3 Experiment 3: ARSI 2017-10-16

This experiment were carried out in Scenario I on October 16th 2017 in Mercat del Born, Barcelona. The dataset includes three missions (i.e. MAV flights) along the following streets: Carrer Fusina, Carrer de la Ribera and Passatge Mercantil. Figure 18 represents the baseline trajectories of the three missions.

- **Carrer Fusina**: The ARSI MAV and router were deployed at manhole *MH Fusina 1* in Figure 13. The inspection follows Carrer Fusina then turns into Passeig de Picasso, flying underneath a service pipe crossing the tunnel. The MAV landed at manhole *MH Passeig 4*. The approximate length of the mission is 50m and the section type is T164 in Fusina streen then T133 when reaching Passeig Colom (see Figure 14).
- **Carrer de la Ribera**: The ARSI MAV and router were deployed at manhole *MH Ribera 3* in figure 13. The inspection follows Carrer de la Ribera, past the intersection with Carrer Comercial on the right, and the MAV lands shortly after manhole *MH Ribera 1*. The approximate length of the mission is 90m and the section type is NT120A then T181.
- **Passatge Mercantil**: The ARSI MAV and router were deployed at manhole *MH Passatge 1* in Figure 13. The inspection follows Passatge Mercantil, and joins Carrer Comercial where the MAV landed at manhole *MH Comercial 3*. The total length of the mission is 47m approx. and the section type is T133.

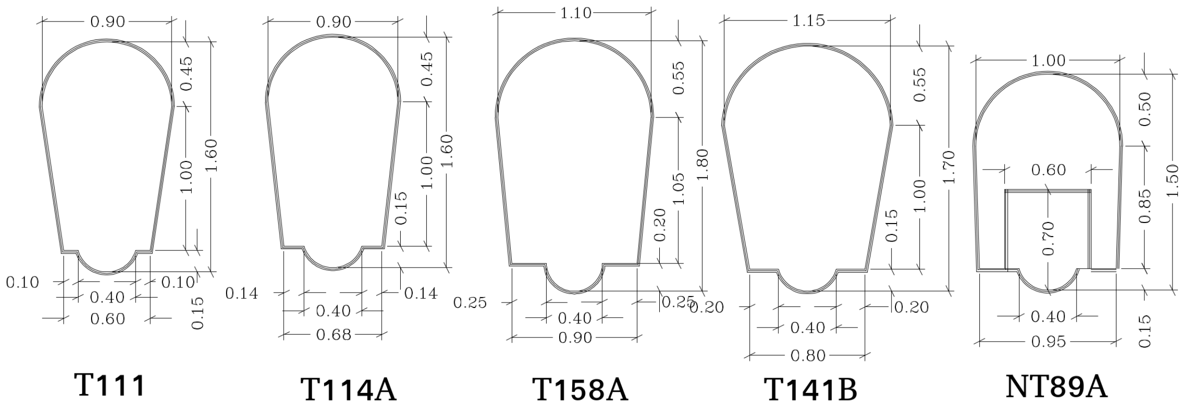

Figure 16: Main cross sections in the Virrei Amat scenario.

Figure 17: Baseline trajectories for experiments 1 (left) and 2 (right).

6.5.4 Experiment 4: SIAR 2017-10-17

In this experiment, the whole track of Scenario I was visited in one hour and twenty five minutes. The platform was guided from the surface. The platform had to be recovered one when visiting Fusina street while acquiring details on a region of interest. Figure 13 represents the baseline trajectory of this experiment in a red line.

6.5.5 Experiment 5: ARSI 2018-07-03

This experiment was carried out in Scenario II. The router and the MAV were deployed at the manhole marked in the as MH 37. Figure 19 depicts the baseline trajectory of the ARSI platform.

6.5.6 Experiment 6: SIAR 2018-07-04

In this experiment we inspected the Virrei Amat Square area (Scenario II) with the SIAR platform. Due to technical issues, the recording of the data had to be split into four different files that lasted almost three hours together. The baseline trajectory related to each part of the experiments is represented in Figure 15. We achieved the inspection over the whole area, visting more than 500m of sewers.

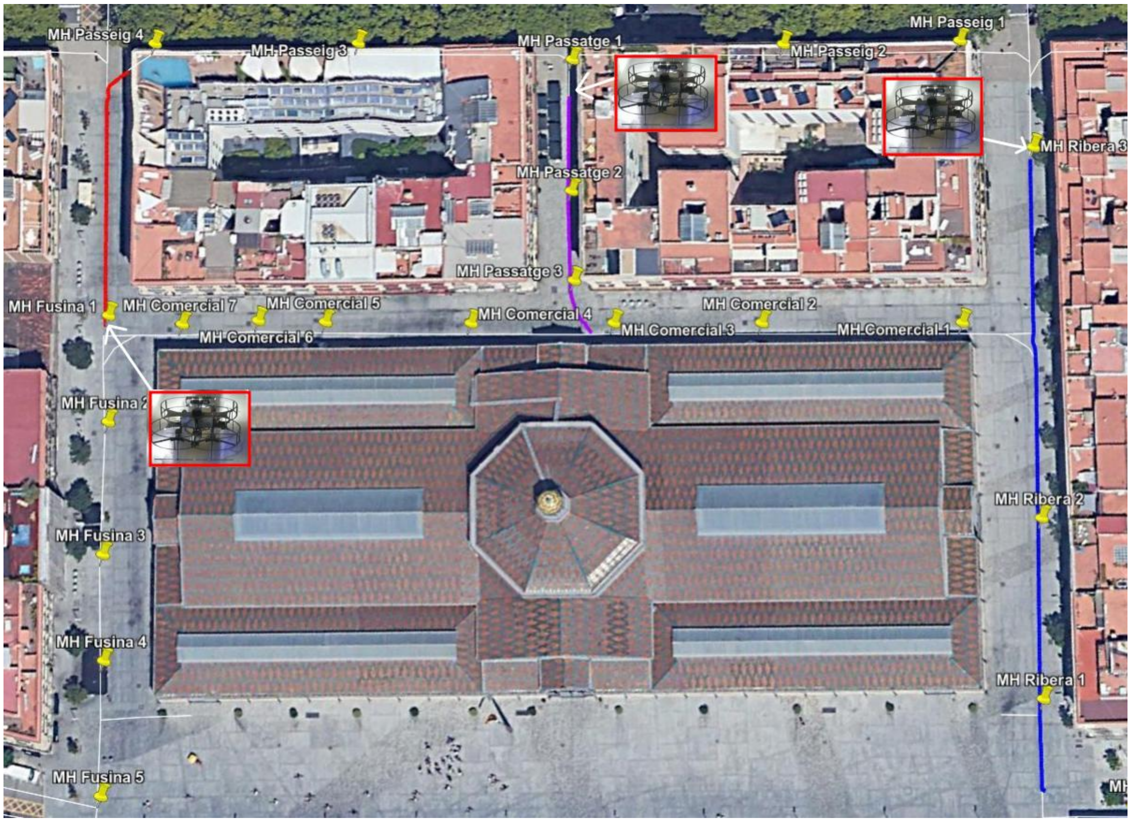

Figure 18: Baseline trajectories of the experiments of the ARSI platform in Scenario 1 (Mercat del Born). The trajectories of Fusina street, Ribera street and Passatge Mercantil are represented in red, blue and purple lines, respectively.

7 Conclusion

In this paper, we provided a detailed description of the dataset generated in the context of the Echord++ PDTI Challenge on Urban Robotics. The dataset include recordings from two different platforms: the aerial platform ARSI and the ground platform SIAR.

The dataset includes accurate baseline trajectories of the platforms that were obtained by taking into consideration the GIS data. In our view, this provides the users with a great understanding of the collected data and can make it a convenient tool for developing SLAM algorithms in confined spaces.

We would like to highlight that the dataset presented here has been obtained over the course of several years of field experimentation inside real sewers of Barcelona. Thanks to this experience we learned several lessons that can be summarized as follows:

- **Plan in advance**. The GIS information available should be carefully studied prior to the experiments. This includes the length of the track to be inspected, the topology of the network and the different cross sections that should be visited. However, bear in mind that the GIS information is generally not very accurate, in particular in old areas. Likewise, be prepared and anticipate any unforeseen situation or unexpected event as it takes a lot of effort to organize the logistics and safety of these operations and it quickly becomes stressful to have the entire logistics team waiting while debugging or changing configurations.

Figure 19: Baseline trajectories of the experiments of the ARSI platform in Scenario II (Virrei Amat).

- **Take care of communications**. At each scenario, we made a field study of the coverage of the deployed communication systems before inserting the robotic platforms. In this way we can determine whether we will be able to provide it with coverage over all the length of the track and the points were the signal is weaker in advance.

- **Continuously test the sensing devices**. This applies to both platforms, but is critical in the operation of an aerial platform. The sensors onboard the platforms should be checked not only at the beginning of the experiments, but a watchdog should be installed to check their integrity in real time. In this way, we can automatically command an emergency landing whenever a critical system is not performing well. In addition, you should take a look on the quality of the data gathered by each sensor before starting a experiment, as the testing conditions may significantly vary from one location to another.

Future work includes providing the user with more reference tools in order to better understand the obtained data. In this way, we are planning to provide reference 3D reconstruction of the environments on each experiment and/or scenario. Moreover, we would also like to enlarge the dataset with the results obtained in additional experiments with both the ARSI and SIAR platforms.

Acknowledgments

This work has received funding from the European Unions Seventh Framework Programme for research, technological development and demonstration under the EU ECHORD++ Project with grant agreement No. 601116. The work at Eurecat was also partially supported by the funding agreement between Eurecat Technology Center and the Catalan Agency for Business Competitiveness (ACCIÓ) for the period 2017-2018. The work at University Pablo de Olavide is also partially supported by the Spanish Ministry of Science, Innovation and Universities (Project COMCISE RTI2018-100847-B-C22, MCIU/AEI/FEDER, UE). D. Alejo is partially supported by the Spanish Ministry of Science and Innovations Juan de la Cierva programme (Ref. FJCI-2015-25700).

The authors would like to thank Mrs. Lina Martinez, Mr. Raul Hernandez and their teams from BCASA (Barcelona Cicle de L'Aigua) and FCC (Fomento de Construcciones y Contratas), respectively, for their logistic support during the field tests. Also, thanks to our colleagues Mr. Paulo Alvito and Mr. Carlos Marques, from IDMind, for designing and building the great SIAR platform and for their priceless help during the field tests. And, in general, thanks to all members of each consortium that supported this work one way or another.

References

Alejo, D., Caballero, F., and Merino, L. (2017). Rgbd-based robot localization in sewer networks. In *2017 IEEE/RSJ International Conference on Intelligent Robots and Systems (IROS)*, pages 4070–4076.

Alejo, D., Chataigner, F., Serrano, D., Merino, L., and Caballero, F. (2019). Into the dirt: Datasets of sewer networks with aerial and ground platforms. `https://robotics.upo.es/datasets/echord`. Accessed: 2019-06-24.

Alejo, D., Marques, C., Caballero, F., Alvito, P., and Merino, L. (2016). Siar: an autonomous ground robot for sewer inspection. In *Actas de las Jornadas de Automática*, pages 1–8.

Avetisyan, R., Willert, M., Ohl, S., and Staadt, O. G. (2014). Calibration of depth camera arrays. In *SIGRAD*.

Balta, H., Bedkowski, J., Govindaraj, S., Majek, K., Musialik, P., Serrano, D., Alexis, K., Siegwart, R., and Cubber, G. (2017). Integrated data management for a fleet of search-and-rescue robots. *J. Field Robot.*, 34(3):539–582.

Blanco, J.-L., Moreno, F.-A., and Gonzalez, J. (2009). A collection of outdoor robotic datasets with centimeter-accuracy ground truth. *Autonomous Robots*, 27(4):327.

Burri, M., Nikolic, J., Gohl, P., Schneider, T., Rehder, J., Omari, S., Achtelik, M., and Siegwart, R. (2016). The euroc micro aerial vehicle datasets. *The International Journal of Robotics Research*, 35.

Fernández-Moral, E., González-Jiménez, J., Rives, P., and Arévalo, V. (2014). Extrinsic calibration of a set of range cameras in 5 seconds without pattern. In *2014 IEEE/RSJ International Conference on Intelligent Robots and Systems*, pages 429–435.

Geiger, A., Lenz, P., Stiller, C., and Urtasun, R. (2013). Vision meets robotics: The kitti dataset. *International Journal of Robotics Research (IJRR)*.

Handa, A., Whelan, T., McDonald, J., and Davison, A. J. (2014). A benchmark for rgb-d visual odometry, 3d reconstruction and slam. In *2014 IEEE International Conference on Robotics and Automation (ICRA)*, pages 1524–1531.

Heng, L., Furgale, P., and Pollefeys, M. (2015). Leveraging image-based localization for infrastructure-based calibration of a multi-camera rig. *Journal of Field Robotics*, 32(5):775–802.

Labb, M. and Michaud, F. (2018). Rtab-map as an open-source lidar and visual simultaneous localization and mapping library for large-scale and long-term online operation: Labb and michaud. *Journal of Field Robotics*.

Leingartner, M., Maurer, J., Ferrein, A., and Steinbauer, G. (2016). Evaluation of sensors and mapping approaches for disasters in tunnels. *Journal of Field Robotics*, 33(8):1037–1057.

Maddern, W., Pascoe, G., Linegar, C., and Newman, P. (2017). 1 Year, 1000km: The Oxford RobotCar Dataset. *The International Journal of Robotics Research (IJRR)*, 36(1):3–15.

Majdik, A., Till, C., and Scaramuzza, D. (2017). The zurich urban micro aerial vehicle dataset. *The International Journal of Robotics Research*, 36:027836491770223.

Meier, L., Honegger, D., and Pollefeys, M. (2015). Px4: A node-based multithreaded open source robotics framework for deeply embedded platforms. *Proceedings - IEEE International Conference on Robotics and Automation*, 2015:6235–6240.

Meier, L., Tanskanen, P., Fraundorfer, F., and Pollefeys, M. (2011). Pixhawk: A system for autonomous flight using onboard computer vision. pages 2992–2997.

Nathan Silberman, Derek Hoiem, P. K. and Fergus, R. (2012). Indoor segmentation and support inference from rgbd images. In *ECCV*.

Pellenz, J., Lang, D., Neuhaus, F., and Paulus, D. (2010). Real-time 3d mapping of rough terrain: A field report from disaster city. In *2010 IEEE Safety Security and Rescue Robotics*, pages 1–6.

Ramón-Vigo, R., Pérez, J., Caballero, F., and Merino, L. (2014). Navigating among people in crowded environment: Datasets for localization and human robot interaction. In *Proceedings of the Workshop on Robots in Clutter: Perception and Interaction in Clutter, IEEE/RSJ International Conference on Intelligent Robots and Systems (IROS)*.

Rizzo, C., Cavestany, P., Chataigner, F., Soler, M., Moreno, G., Serrano, D., Lera, F., and Villarroel, J. L. (2018). Wireless propagation characterization of underground sewers towards autonomous inspections with drones. In *ROBOT 2017: Third Iberian Robotics Conference*, pages 849–860.

Schneider, S., Luettel, T., and Wuensche, H.-J. (2013). Odometry-based online extrinsic sensor calibration. In *2013 IEEE/RSJ International Conference on Intelligent Robots and Systems*, pages 1287–1292.

Smisek, J., Jancosek, M., and Pajdla, T. (2013). *3D with Kinect*, pages 3–25. Springer London, London.

Sturm, J., Burgard, W., and Cremers, D. (2012). Evaluating egomotion and structure-from-motion approaches using the TUM RGB-D benchmark. In *Proc. of the Workshop on Color-Depth Camera Fusion in Robotics at the IEEE/RJS International Conference on Intelligent Robot Systems (IROS)*.

A Custom datatypes for SIAR platform

Even though most of the information of the rosbag files presented in this paper uses standard types from the ROS base libraries, we opted to generate custom messages to group internal messages for introspective information of the SIAR platform. In this appendix, the information about our custom types is detailed.

- `siar_driver/SiarStatus`. This topic contains information of the complete status of the platform. It includes information of the internal status of the platform, including raw odometry values, the status of width adjustment motors, the servos of the arm and the onboard lights. In addition, it provides information about the remaining battery and about the power supply, if connected. Below you can find the fields included in the topic:

std_msgs/Header header	float32 electronics_x	float64 x
string motor_fw_version	float32 width	float64 y
string battery_fw_version	int64 front_left_ticks	float64 speed
int8 operation_mode	int64 front_right_ticks	siar_driver/SiarBatteryMonitor elec_battery
bool reverse	int64 middle_left_ticks	siar_driver/SiarBatteryMonitor motor_battery
bool slow	int64 middle_right_ticks	siar_driver/SiarPowerSupply power_supply
bool fan	int64 back_left_ticks	bool front_light
bool hard_stop	int64 back_right_ticks	bool rear_light
bool is_stopped	int16[5] herculex_position	uint8 aux_pins_values
uint8 hard_stop_time	uint8[5] herculex_temperature	nav_msgs/Odometry odom
uint16 lin_motor_pos	uint8[5] herculex_status	bool arm_panic
uint16 lin_motor_pot	uint8[5] herculex_torque	

- `siar_driver/SiarBatteryMonitor`. This topic groups the information of the sensors for battery monitoring.

float32 voltage	float32 current	float32 integrated_current
int8 percentage	int16 remaining_time	

- `rssi_get/Nvip_status`. This message has information about the communication link established between the onboard communication systems and the deployed communication systems.

string mac	int8 rssi_perc	float32 rx_rate
int8 rssi	float32 tx_rate	

- `amcl_sewer/Manhole`. This message has information related to the position of a detected manhole. It is used in the dataset to indicate the precise instant when the SIAR platform passed below a manhole. It can be used as partial ground truth to test localization systems.

int32 id	geometry_msgs/Pose2D local_position	nav_msgs/NavSatFix gps_position

- `libelium_waspmote_gas_node/GasMeasure`. Includes all the information related to one measurement of the gas sensor onboard the SIAR platform.

std_msgs/Header head	float32 O2_conc	bool O2_alarm
int32 time	float32 H2S_conc	bool H2S_alarm
int8 bat_perc	float32 CO_conc	bool CO_alarm
float32 bat_level	float32 CH4_conc	bool CH4_alarm
float32 temperature	float32 pressure	float32 RH
geometry_msgs/Vector3 accel		